

## Articles

# Statistical Analysis of Single-Molecule Colocalization Assays

W. Trapesinger,<sup>\*,†</sup> B. Hecht,<sup>†</sup> U. P. Wild,<sup>†</sup> G. J. Schütz,<sup>‡</sup> H. Schindler,<sup>‡</sup> and Th. Schmidt<sup>§</sup>

Institute for Physical Chemistry, ETH Zürich, CH-8092 Switzerland, Institute for Biophysics, University of Linz, A-4040 Linz, Austria, and Huygens Laboratory, University of Leiden, P.O. Box 9504, 2300 RA Leiden, Netherlands

**In chemical assays, specific molecular recognition events result in close physical proximity of two molecular species, e.g., ligands and receptors. Microscopy techniques that are able to image individual molecules allow for achieving a positional accuracy far beyond the resolution limit. Therefore, independent position determination, e.g., by dual-color microscopy, becomes possible, permitting determination of intermolecular distances beyond the resolution limit. Nonzero measured distances occur due to experimental inaccuracies in case of a recognition event or due to accidental close proximity between ligand–receptor pairs. Using general statistical considerations, finite measured distances between single ligand–receptor pairs are directly translated into probabilities for true molecular recognition or mere accidental proximity. This enables a quantitative statistical analysis of single recognition events. It is demonstrated that in a general assay, even in the presence of strong unspecific background, the probability for a certain diagnosis and a measure for its reliability can be extracted from the observation of a few binding events. The power of the method is demonstrated at the example of a single-molecule DNA hybridization assay. Our findings are of major importance for future assay miniaturization and assaying with minute amounts of analyte.**

A frequent problem in analytical assays is that usually small quantities of analyte are to be detected with highest reliability in the presence of a multitude of other, often unknown substances. Therefore, for example, fluorescence, absorption, or radioactivity due to specific binding between a ligand and a receptor has to be discriminated from a respective unspecific background. To account for the background, conventional techniques rely on reference measurements to quantify the amount of unspecific signal.<sup>1</sup> For assays with ever smaller quantities of reagents, this strategy ceases to be meaningful when the uncertainty in background

determination exceeds the signal due to specific recognition, thus setting a lower limit for the precise quantification of amounts of substance. This inherent problem can be overcome, for example, by applying an assay architecture where specific binding is detected, by monitoring signals exclusively due to the close proximity of ligand and receptor.<sup>2–5</sup>

A key advantage of single-molecule techniques is their ability to circumvent averaging. Hence it becomes possible to unravel correlations of individual events rather than detecting changes of average values.<sup>6,7</sup> With respect to analytical applications, this means that probabilities for the occurrence of an event of interest can be quantified on a single-event basis.<sup>8</sup> The introduction of quantitative single-molecule assays to applied analytical chemistry thus should result in important improvements, since the detection of minute quantities of substances accompanied by a strong background becomes feasible, making realistic applications in forensics or environmental protection conceivable.<sup>9–12</sup> The increased experimental efforts associated with single-molecule techniques can be justified for two reasons: (i) diagnosing a disease at an early stage, where examination of only a small amount of tissue taken from a patient needs to yield unambiguous results;<sup>12</sup> to a similar extent, (ii) developments toward increased throughput of screening methods or the miniaturization of assays call for the detection of minute quantities of analyte leading to digital chemical analysis in the ultimate limit.

We introduce a general statistical approach for the evaluation of colocalization assays by dual-color single-molecule imaging. On the basis of the very high spatial accuracy achieved in single-

\* To whom correspondence should be addressed: (e-mail) wtrape@phys.chem.ethz.ch.

<sup>†</sup> ETH Zürich.

<sup>‡</sup> University of Linz.

<sup>§</sup> University of Leiden.

(1) Mayer, A.; Neuenhofer, S. *Angew. Chem., Int. Ed. Engl.* **1994**, *33*, 1044–1072.

(2) Förster, T. *Ann. Phys.* **1947**, *2*, 55–75.

(3) Nryer, L.; Haugland, R. P. *Proc. Natl. Acad. Sci. U.S.A.* **1967**, *58*, 719–726.

(4) Castro, A.; Williams, J. G. K. *Anal. Chem.* **1997**, *69*, 3915–3920.

(5) Kettling, U.; Koltermann, A.; Schwill, P.; Eigen, M. *Proc. Natl. Acad. Sci. U.S.A.* **1998**, *95*, 1416–1420.

(6) *Frontiers in Chemistry: Single Molecules. Science* **1999**, *283*.

(7) Basche, T.; Moerner, W. E.; Orrit, M.; Wild, U. P. *Single-molecule optical detection, imaging and spectroscopy*; VCH: Weinheim, Germany, 1997.

(8) Lu, H. P.; Xun, L.; Xie, X. S. *Science* **1998**, *282*, 1877–1882.

(9) Eigen, M.; Rigler, R. *Proc. Natl. Acad. Sci. U.S.A.* **1994**, *91*, 5740–5747.

(10) Rigler, R. *J. Biotechnol.* **1995**, *41*, 177–186.

(11) Trapesinger, W.; Schütz, G. J.; Gruber, H. J.; Schindler, H.; Schmidt, T. *Anal. Chem.* **1999**, *71*, 279–283.

(12) Ng, K. C.; Whitten, W. B.; Arnold, S.; Ramsey, J. M. *Anal. Chem.* **1992**, *64*, 2914–2919.

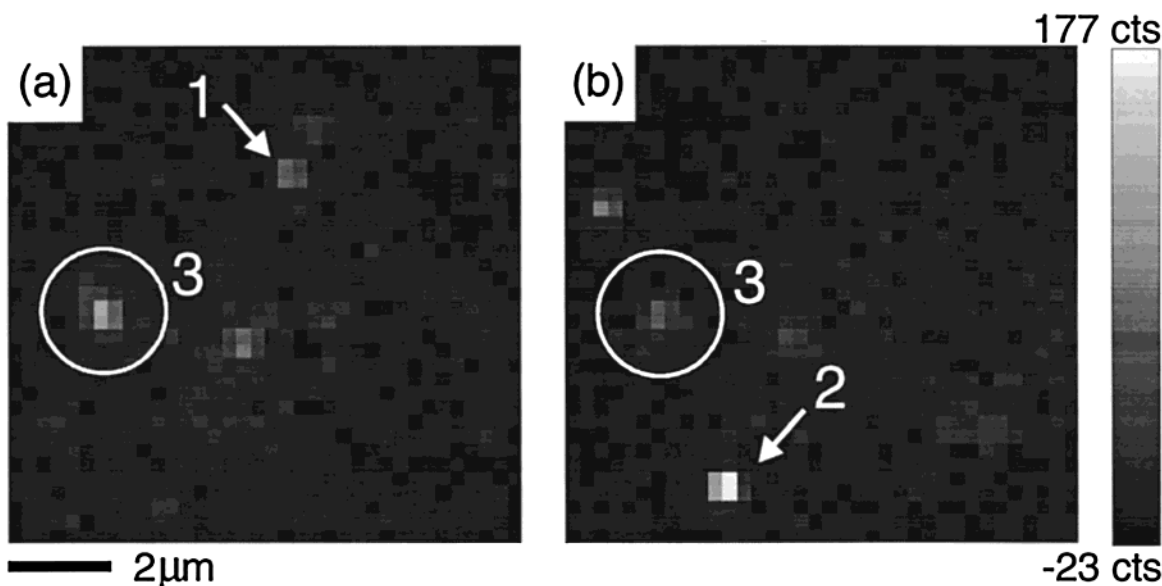


Figure 1. Dual-color exposures taken during a single-molecule hybridization experiment. Image a obtained by green illumination shows the distribution of green-labeled receptor molecules, image b the distribution of red-labeled ligand molecules. Comparison of the red and green exposures shows all three possible events: (1) isolated green receptor molecules, (2) isolated red ligand molecules, and (3) ligand and receptor molecules at coincident positions (indicated by the circles).

molecule imaging,<sup>11,13–17</sup> we determine distances between individual immobilized ligand–receptor pairs<sup>11,14</sup> well below the resolution limit. The ensemble of pairs is composed of two distinct subsets: in addition to those pairs that are actually bound, ligands and receptors can also be found in close proximity at random due to unspecific adsorption to the surface. Starting from well-known expressions for the distributions of distances in either case, we construct a measure for the probability of correct assignment of a single receptor–ligand pair as a function of its detected intermolecular distance.

To demonstrate the power of the present approach, we apply our method to the analysis of a single-molecule DNA hybridization assay described previously.<sup>11</sup> In contrast to our previous findings, where a diagnosis was made on the basis of 289 observations, we now find that a few observations suffice to confidently establish a diagnosis based on a predefined quantitative criterion.

## EXPERIMENTAL SECTION

**Materials.** The substrate consisted of a phospholipid bilayer deposited onto a clean microscopy cover slip. Immobilization of single-stranded DNA target sequences to the substrates was performed via biotin–streptavidin linkage, where the streptavidin molecules were labeled for green excitation. In contrast, complementary single-stranded DNA probe sequences were labeled for red excitation. After the substrate preparation procedure, the red-labeled probe sequences were allowed to bind to the green-labeled target sequences during a 10-min incubation period, followed by thorough washing steps to expel unbound probes from the

surface. For a more detailed description of the preparation procedures, see ref 11.

**Microscopy.** A dual-color single-molecule microscopy setup previously described in detail<sup>14</sup> was used to sequentially acquire images showing the spatial distribution of red and green molecules, respectively. Careful calibration of the apparatus excluded systematic sources of error, such as vibrations and chromatic aberrations, demonstrating that red and green microscopy images are in accurate spatial registry. The fluorescence pattern observed for a single molecule can be fitted to a two-dimensional Gaussian, precisely revealing the lateral position of the molecule. A series of test measurements with dual-color labeled single molecules,<sup>14</sup> followed by a fitting procedure proved an accuracy of 38 nm for measuring the distance between red and green molecules. Figure 1 shows single-molecule fluorescence images obtained in the hybridization assay. Two images taken at the same sample spot in sequence show the distribution of red- and green-labeled molecules, respectively.

## THEORY

After running a binding assay with fluorescence-labeled molecules, a concentration  $c_R$  of molecules of species R (ligand molecules; here, DNA probe sequences) and a concentration  $c_G$  of molecules of species G (receptor molecules; here, DNA target sequences), respectively, are found immobilized on a surface. R indicates labeling for red, G for green excitation, respectively. Three different types of events may be distinguished: (1) isolated green receptor molecules, (2) isolated red ligand molecules that are unspecifically adsorbed to the surface, and (3) specific binding events, characterized by red and green spots, i.e., ligand and receptor molecules in close proximity, as indicated by the circles in Figure 1.

There are two distinct cases for the observation of a ligand R: (i) a ligand molecule R which is specifically bound to a receptor G (probability  $p(s)$ ,  $s$  for specific binding) and, (ii), a molecule R

(13) Bobroff, N. *Rev. Sci. Instrum.* **1986**, *57*, 1152–1157.

(14) Schütz, G. J.; Trabesinger, W.; Schmidt, Th. *Biophys. J.* **1998**, *74*, 2223–2226.

(15) Betzig, E. *Opt. Lett.* **1995**, *20*, 237–239.

(16) van Oijen, A. M.; Köhler, J.; Schmidt, J.; Müller, M.; Brakenhoff, G. J. *Chem. Phys. Lett.* **1998**, *292*, 183.

(17) Lacoste, T. D.; Michalet, X.; Pinaud, F.; Chemla, D. S.; Alivisatos, A. P.; Weiss, S. *Proc. Natl. Acad. Sci. U.S.A.* **2000**, *97*, 9461–9466.

unspecifically adsorbed to the surface ( $p(u) = 1 - p(s)$ ,  $u$  for unspecific binding). The probabilities  $p(s)$  and  $p(u)$  can be determined straightforwardly from an ensemble measurement of specific or unspecific binding. In practice, this is done by performing binding experiments with two substrates, one with receptors, one without receptors. On average, there are  $p(s)c_R$  R–G pairs per surface unit due to molecular recognition events, where  $c_R$  is the surface density of R molecules. All the remaining  $p(u)c_R$  R molecules that do not belong to the abovementioned pairs are unspecifically adsorbed on the surface (if, as in our case, there are less receptors (G) than ligands (R)). The goal of our analysis is to calculate molecular recognition probabilities for all pairs on a one-by-one basis. To arrive at a quantitative description, we pursue the following strategy: From first principles, we derive conditional probabilities for observing certain intermolecular R–G distances given the assumption that the molecules are specifically (unspecifically) bound to the substrate. Exploiting the knowledge of  $p(s)$  and  $p(u)$ , we can then assign probabilities for specific (unspecific) binding given a certain measured intermolecular distance for an individual pair of R and G molecules.

To provide a basis for the analysis of our data, we use a simple computer algorithm to generate an ideal assignment of R–G pairs found in images. The algorithm is devised such that it finds the most likely out of all possible pair assignments, i.e., the one for which the sum of all intrapair R–G distances is minimal. This provides a list of distances  $r'$  between the assigned R–G pairs. For our analysis, we start from a probability density function (pdf) for the intermolecular distances of an R–G pair in Cartesian coordinates,

$$\rho(\delta x, \delta y) dx dy \propto \exp\left(-\frac{(\delta x - \Delta x)^2 + (\delta y - \Delta y)^2}{4\sigma^2}\right) dx dy \quad (1)$$

which is simply a two-dimensional Gaussian distribution reflecting the measurement uncertainties centered around the actual distance  $\Delta x$  in the  $x$ -direction and  $\Delta y$  in the  $y$ -direction, respectively. Here,  $\sigma$  is the standard deviation of the microscope for locating the position of a molecule, which can be determined independently.<sup>13</sup> Since, for the present purposes, rotational symmetry can be assumed, the above expression is transformed to polar coordinates, and integration over all polar angles is performed. This yields the following pdf:

$$\rho(r'|r) dr' = \frac{1}{2\sigma^2} r' \exp\left(-\frac{r^2 + r'^2}{4\sigma^2}\right) I_0\left(\frac{rr'}{2\sigma^2}\right) dr' \quad (2)$$

where  $r$  denotes the actual physical distance between two molecules,  $r'$  is the measured intramolecular distance, and  $I_0$  is the zero-order modified Bessel function of the first kind. The function  $\rho(r'|r) dr'$  (eq 2) describes the probability to measure a distance  $r'$  between a R–G pair given that the actual distance is  $r$ . This pdf fully characterizes the distribution of intermolecular distances that would be obtained from repeated distance measurements on one and the same pair of molecules. For the special case of specific binding (case s) between two molecules, the pdf of the measured distance  $r'$  is obtained from eq 2 by setting  $r = 0$  yielding

$$\rho(r'|s) dr' = \frac{1}{\sigma^2} r' \exp\left(-\frac{r'^2}{4\sigma^2}\right) dr' \quad (3)$$

Assuming a random distribution of molecules, one can also derive an expression for the pdf for incidental proximity (case u) of an unspecifically adsorbed molecule R to a molecule G:<sup>18</sup>

$$\rho(r|u) dr = 2\pi p(u) c_R \exp(-r^2 \pi p(u) c_R) dr \quad (4)$$

To account for the measurement uncertainty in determining intermolecular distances, this pdf has to be convolved with the expression for  $\rho(r'|r)$  (eq 2), yielding

$$\rho(r'|u) = \int \rho(r'|r) \rho(r|u) dr = \frac{2\sigma^2}{1 + 4\pi p(u) c_R \sigma^2} \exp\left(-\frac{r'^2 \pi p(u) c_R}{1 + 4\pi p(u) c_R \sigma^2}\right) \quad (5)$$

The quantities of interest for our purposes are  $p(s|r')$  and  $p(u|r')$  =  $1 - p(s|r')$ , the probabilities for specific binding or incidental vicinity given the measured distance  $r'$ . Above, we have derived  $\rho(r'|s)$  and  $\rho(r'|u)$ , which are related to the desired function  $p(s|r')$  by Bayes' theorem:<sup>19</sup>

$$p(s|r') = \frac{p(s)\rho(r'|s)}{p(s)\rho(r'|s) + p(u)\rho(r'|u)} \quad (6)$$

The function  $p(s|r')$  is found by substituting eqs 3 and 5 into eq 6. Thus, it is possible to generate a “look-up table” that can be consulted to assign a probability for specific binding to each measured distance. The possibility to refer to a look-up table is instrumental for the kind of fast analysis ultimately needed in a screening assay.<sup>20</sup> Figure 2 shows the typical behavior of the look-up table  $p(s|r')$  for the set of parameters given in the figure caption. The function  $p(s|r')$ , corresponding to the DNA wide-field experiment, is plotted as a solid line. As is evident, for distances larger than 200 nm the probability for specific binding is negligible. The dashed line holds if, for example, near-field optical microscopy was used to image the molecules. It is evident that the increase in spatial resolution results in a significantly improved statistical confidence for discriminating specific binding events.

## RESULTS AND DISCUSSION

Figure 3 shows a probability series obtained for all 289 pairs of molecules found in the DNA hybridization experiment. The probabilities were obtained from the set of measured R–G distances using the look-up table (eq 6) plotted in Figure 2. Most strikingly, we observe that the 289 pairs are clearly divided into two distinct categories: (i) those that exhibit values of  $p(s|r')$  close to zero (94%) and (ii) those that have high  $p(s|r')$  values, indicating high probabilities for specific binding (6%). This finding is a clear result of the sigmoidal shape of the look-up table in Figure 2. The

(18) Chandrasekhar, S. *Rev. Mod. Phys.* **1943**, *15*, 1.

(19) Papoulis, A. *Probability, Random Variables, and Stochastic Processes*; McGraw-Hill: New York, 1992.

(20) Prummer, M.; Hübner, C. G.; Sick, B.; Hecht, B.; Renn, A.; Wild, U. P. *Anal. Chem.* **2000**, *72*, 443–447.

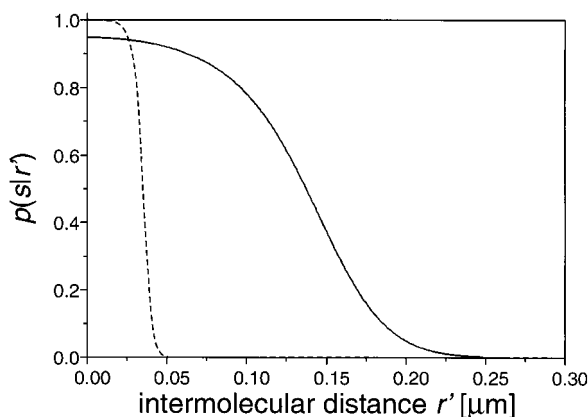


Figure 2. Colocalization probability vs measured intermolecular distance. The clearly sigmoidal shape of both curves shows that a very sharp distinction between incidental vicinity of molecules and specific binding is possible. The solid line is obtained for the experimental parameters of our wide-field fluorescence microscopy experiment ( $p(s) = 0.05$ ,  $\sigma = 30$  nm,  $c_R = 0.1 \mu\text{m}^{-2}$ ), whereas the dashed line holds for typical apparatus parameters in near-field microscopy ( $p(s) = 0.05$ ,  $\sigma = 5$  nm,  $c_R = 0.1 \mu\text{m}^{-2}$ ).

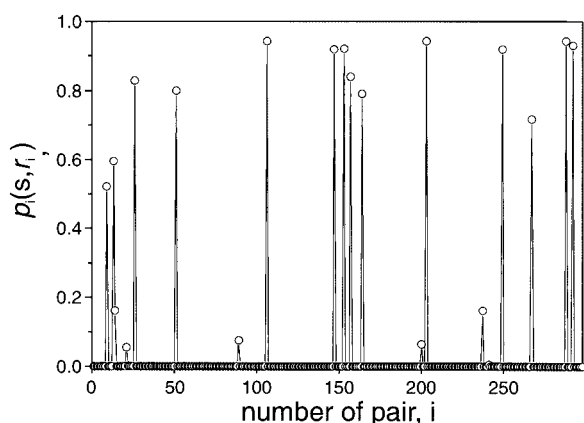


Figure 3. Probability series obtained for all pairs of molecules obtained in the experiment. These probabilities were obtained by applying the function depicted in Figure 2 to the set of measured intermolecular distances. Almost all events can either be discarded as unspecific (points close to zero) or show a very high probability for true molecular recognition.

use of a higher resolution microscopy would lead to even more distinct results. We want to point out that the continuous function used as look-up table permits an objective quantification of the probability for specific binding for any measured intermolecular distance.

In our previous analysis,<sup>11</sup> we took the simplified assumption that specific binding had occurred in cases where intermolecular distances smaller than  $\sigma$  were measured. In view of the present analysis, this corresponds to approximating the look-up table derived here by a radial step function. The drawback of this simple approach is that the assignment of results is purely binary and that there is no quantitative value for the likelihood of an error. Therefore, the previous work had to rely on all 289 events in order to arrive at a conclusion about the single-molecule colocalization assay.<sup>11</sup> In contrast, the present methodology, while being consistent with the step function approach, permits the full statistical description of a *single* observation, i.e., the probability for the truth of a given hypothesis (i.e., “specific recognition has occurred”) can be quantified accurately.

Up to this point, we have shown that single pairing events can be characterized quantitatively. However, when analyzing the outcome of a single-molecule colocalization assay, we will in general have to deal with multiple events, i.e., a small set of pairing events. It is a challenge with respect to diagnostic applications to come up with a statistically sound method that enables us to make decisions on the basis of a small set of observations. For a reliable judgment, it should be possible to calculate the probability that no recognition took place, which, for example, in medical applications would correspond to a negative diagnosis. From a naive point of view, this is easy to accomplish: Multiplying the values of  $p_i(u|r')$  of all observed pairs yields the probability

$$p_0 = \prod_i p_i(u|r') \quad (7)$$

that *all* individual pairing events were unspecific corresponding to the probability for a negative outcome of the assay. Although this simple consideration is correct, it may be misleading. This can be demonstrated at the example of a worst-case scenario consisting of a hypothetical experiment in which every individual pairing event is characterized by  $p_i(u|r') = p_i(s|r') = 0.5$ . Because there is equal probability for both, recognition and unspecific binding, this experiment evidently does not provide any information! Judging from eq 7, however, one would conclude based on only seven observations that the probability for a negative outcome of the assay is less than 1%. From this consideration, it is obvious that additional information is required in order to establish a *reliable* diagnosis. We therefore suggest a more complete characterization of the experiment. A diagnosis based on the assay should rely on *two* characteristic figures: (i) the probability that the outcome of the assay is negative, which is provided by  $p_0$ , eq 7, and (ii) the quality of the measurement in comparison to other measurements (and hence, how reliable is the value determined in (i)).

To establish both, a measure of reliability and the desired value for the probability that the outcome of the assay was negative, we propose the following strategy: Having observed  $N$  individual pairs in an experiment, a set of probabilities  $\{p_1(s|r'_1), p_2(s|r'_2), \dots, p_N(s|r'_N)\}$  is obtained. The experiment is completely characterized by specifying the probabilities for all possible outcomes, i.e., the  $N$  probabilities  $p_m$  for the truth of the statements: “ $m \leq N$  events out of  $N$  pairs observed in total were due to specific recognition”. These probabilities are obtained by applying similar considerations that lead to the binomial distribution. However, in contrast to a binomial distribution, which would be determined by only two *constant* probabilities  $p(u|r')$  and  $p(s|r')$  applying to each of the  $N$  individual events, we have to consider the more general case, where each event is characterized by different probabilities  $p_i(u|r'_i)$  and  $p_i(s|r'_i)$ . We thus combine the probability values assigned to each individual pair of molecules (eq 6) to generate the discrete probabilities  $p_m$ . To obtain the  $p_m$ , we apply a combinatorial algorithm that generates all possible outcomes of the experiment with their respective probabilities. If  $S_m$  denotes the set of possibilities  $S_{kn}$ ,  $n \in \{1.. \binom{N}{m}\}$ , of choosing  $m$  values out of the set  $\{p_1(s|r'_1), p_2(s|r'_2), \dots, p_N(s|r'_N)\}$ , and  $\bar{S}_{kn}$  is its complementary set, then

$$p_m = \sum_k \prod_{i \in S_{kn}} p_i(s|r'_i) \prod_{i \in \bar{S}_{kn}} (1 - p_i(s|r'_i)) \quad (8)$$

i.e., the sum over all possible joint probabilities resulting in  $m$  specific recognition events and  $N - m$  incidental events. In other words, if  $p_m$ , the probability for  $m$  specific events, is desired, all possibilities of picking  $m$  pairs out of the entire set of  $N$  have to be considered. For example, in the case  $N = 4$ , where  $n \in \{1 \dots 4\}$ ,  $S_3$  reads as follows:  $S_3 = \{S_{31}, S_{32}, S_{33}, S_{34}\} = \{\{p_1, p_2, p_3\}, \{p_1, p_2, p_4\}, \{p_1, p_3, p_4\}, \{p_2, p_3, p_4\}\}$  and  $\bar{S}_3 = \{S_{31}, \bar{S}_{32}, \bar{S}_{33}, \bar{S}_{34}\} = \{p_4, p_3, p_2, p_1\}$ . For each of the subsets  $S_{kn}$ , one can calculate the joint probability that the events in  $S_{kn}$  were indeed specific binding events, whereas all other  $N - m$  events in  $\bar{S}_{kn}$  were unspecific by forming the product of the respective  $p_i(s|r'_i)$  and  $p_i(u|r'_i) = 1 - p_i(s|r'_i)$ . By summing all of the latter, over the index  $k$ , as is done in eq 8, one arrives at the probability  $p_m$  that any  $m$  pairs out of  $N$  were specific binding events. This distribution represents the most complete characterization of the hybridization experiment that is possible on the basis of the measured data.

The distribution of probabilities  $p_m$  contains the desired diagnosis parameters straightforwardly: (i) The probability that the outcome of the assay is negative is given by  $p_0$ . The quality of the measurement, (ii), is obviously characterized by the width of the distribution of  $p_m$  values. A very narrow, sharply peaked distribution will clearly indicate one distinct outcome of the experiment as most likely, whereas broad distributions yield less information. We define a measure of quality  $q$  that ranges from  $q = 0$  for experiments void of information to  $q = 1$  for ideal experiments, i.e., conditions under which the outcome of the experiment can be assigned unambiguously. Considering again the worst-case experiment discussed above that did not yield any information, a binomial distribution for the probability 0.5 would be obtained for the  $p_m$  values. This worst-case distribution has a standard deviation of  $1/2N^{1/2}$ . Consequently,

$$q = 1 - \frac{2\sigma(p_m)}{\sqrt{N}} \quad (9)$$

fulfills the defined requirements. Here  $\sigma(p_m) = (\sum_i p_i(i - \bar{m})^2)^{1/2}$  is the standard deviation of the distribution of  $p_m$  values, where  $m = \sum_i i p_i$ . The function  $q$  can be used to determine which of various possible experimental assays is best suited for obtaining a diagnosis. Taking into account these two criteria, the relevant conclusions from a given experiment can be drawn: A diagnosis can be obtained with a quantitative, predefined criterion (e.g.,  $p_0$  must be smaller than 1%); the quality of this diagnosis can be quantified by its  $q$  value and thus be compared to other experiments. In our worst-case scenario discussed above we would obtain  $q = 0$ , although  $p_0$  is very small, and consequently, no diagnosis could be given.

To demonstrate this methodology, the total set of 289 measured pairs was randomly split into subsets of 20 pairs. Each of the subsets can be considered as an experiment where we are forced to give a reliable diagnosis based on only few events.

For each of the subsets, the probabilities  $p_m$  were calculated as defined in eq 8. On the left side of Figure 4, the  $p_m$  values obtained for one exemplary subset of 20 pairs are plotted (filled

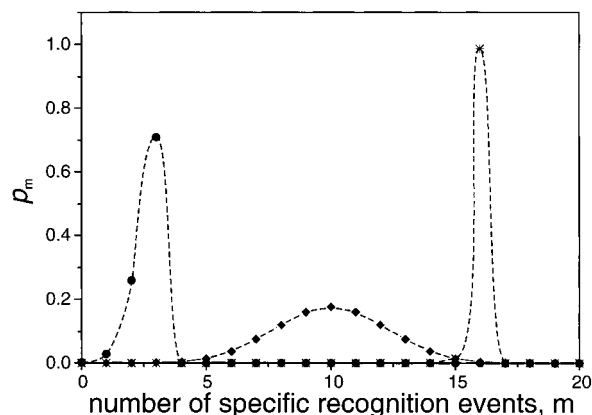


Figure 4. Construction of the probability distribution for each subexperiment after splitting the calculated probabilities into subsets of 20. The curve on the left side of the diagram was obtained during the experiment and shows an almost unambiguous assignment of the number of successful oligonucleotide pairings. The curve on the right side of the diagram is a Monte Carlo simulation of an experiment with very efficient reaction conditions. For comparison, the plot in the center of the diagram would be obtained for an experiment with minimum information content (binomial distribution).

circles). The maximum value of  $p_m$  is found for  $m = 3$ . More importantly, we note that (i)  $p_0 \approx 0$ , indicating a positive outcome of the assay. Furthermore, (ii) the distribution exhibits a small width resulting in a value of  $q$  close to 1 ( $q \approx 0.75$ ), underscoring the reliability of the statement made in (i). The average number of successful binding events deduced from the  $p_m$  reflects the chemical affinity between ligand and receptor. In particular, the experimental  $p_m$  distribution is indicative of low binding affinity, as is evident from the fact that it is centered at  $m = 3$ . For other subsets,  $p_m$  distributions with maximums at different positions but of similar shape are found. Also plotted in Figure 4 is a binomial distribution for the parameter 0.5 as the limiting case for maximum uncertainty (filled diamonds), as well as a Monte Carlo simulation for very efficient (80%) reaction conditions (sharp distribution, peaked at  $m = 16$ , at the right end of the interval, stars). For the present assay it can be seen that in spite of the low binding probability, the narrowness of the  $p_m$  distribution indicates a high statistical reliability of the diagnosis based on a small number of events.

## CONCLUSIONS

In contrast to conventional ensemble assays, where only the total quantity of molecular species present in the detection volume can be measured, our approach additionally takes advantage of spatial information by using intermolecular distance measurements. It is therefore possible to assign probabilities for specific binding and incidental proximity to individual pairs, rendering this methodology significantly more insensitive to unspecific adsorption events. In addition to single-pair analysis, we also demonstrate a statistical methodology that allows for compiling any number of observations into relevant decision criteria. In addition to specifying the probability for the diagnosis that molecular recognition has occurred ( $1 - p_0$ ), another relevant quantity has been deduced, i.e., a quality parameter  $q$ , which constitutes an objective measure for how reliably an experimental method assigns a certain outcome of an experiment as the most likely one. This parameter

not only allows for judging the reliability of a diagnosis but also provides an objective criterion for comparing different microscopy techniques for a certain analytic application. It is therefore possible to terminate an experiment after any number of observations, while a complete statistical characterization of the outcome is still possible. The measurements used to illustrate the potential of our analysis indicate that only few successful binding events are required to establish a reliable diagnosis. In particular, we have demonstrated at the example of an experimental model system that 20 observations suffice for a highly reliable diagnosis. This finding is particularly intriguing in view of the fact that the resolution of the optical wide-field microscopy employed is poor in comparison to molecular-length scales. We therefore believe that the applicability of our method to virtually any type of microscopy and its simplicity may advance highly sensitive parallel

analytical techniques with medical and forensic applications, where strong background suppression is a key requirement.

#### ACKNOWLEDGMENT

We thank Beate Sick and Michael Prummer for discussions on Bayesian statistics. Axel Kramer and Christian Huebner are gratefully acknowledged for careful proofreading of the manuscript. Hermann Gruber is gratefully acknowledged for fluorescence labeling of the oligonucleotides, which were a kind gift of Dr. Hallermayer and Dr. Kleiber from Boehringer Mannheim.

Received for review July 13, 2000. Accepted November 22, 2000.

AC000810T